Exciton Localization in Vertically and Laterally Coupled GaN/AlN Quantum Dots

ARTICLE *in* NANO LETTERS · FEBRUARY 2005

Impact Factor: 13.59 · DOI: 10.1021/nl048511x · Source: PubMed

NANO LETTERS

2005
Vol. 5, No. 2
213−217

Exciton Localization in Vertically and Laterally Coupled GaN/AlN Quantum Dots

A. Neogi*

Department of Physics, University of North Texas, Denton, Texas 76203

H. Morkoç

Department of Electrical Engineering, Virginia Commonwealth University, Richmond, Virginia 23284

T. Kuroda and A. Tackeuchi

Department of Applied Physics, Waseda University, Okubo 3-4-1, Tokyo 169-8555, Japan

T. Kawazoe and M. Ohtsu

Department of Physics, University of Tokyo, Japan

Received September 13, 2004; Revised Manuscript Received December 2, 2004

ABSTRACT

Near-field and time-resolved photoluminescence measurements show evidence of exciton localization in vertically and laterally coupled GaN quantum dots (QDs). The binding energies in multiple period QDs (MQDs) are observed to be stronger by more than six times compared to single period QDs (SQDs). Excitons in MQDs have a short (450 ps) lifetime and persist at room temperature, while SQDs exhibit extraordinarily long (>5 ns) lifetime at 10 K due to reduced spatial overlap of electron and hole wave functions in strained QDs.

The most spectacular property of quantum-confined nitride-based quantum well (QW) or dots (QD) lie in the huge electric fields along their growth axes as this material system normally has wurtzite symmetry.[1−6] The study of nitride QDs is particularly interesting as it depicts the interplay of built-in strain-dependent electric fields and quantum confinement in the nitride-based material system. When the dot size is of the order of the exciton Bohr radius, the quantum confinement effects on both the exciton binding energy and the optical band gap allow tailoring of the optical properties of the system.[3,6] In self-organized GaN QDs, the quantum confinement effect observed in the "classical" GaAs-based QD or QW, is offset by the large piezoelectric and spontaneous polarization fields, resulting in a red shift of the ground-state optical transition below the bulk band gap by about 0.5 eV.[3] This enormous shift is attributed to the piezoelectric field exceeding 5 MV/cm. The dot size and built-in strain fields can be engineered to tune the emission wavelength from the visible to the ultraviolet light regime in GaN-QD based optical emitters. QD layers are expected to effectively decouple the active layers from the substrate and the buffer layer and, thus reduce the defect density.[6]

We have recently reported the growth of GaN QDs grown on relatively thin AlN spacer layers (2 nm). A large blue-shift in the exciton emission energy indicates a strong carrier confinement, despite the reduction in the effective stress within the GaN QD layers.[7−9] In this paper, we compare the carrier recombination dynamics in single period laterally coupled QD (SQD) and multiple period vertically stacked QD (MQD) for investigating the emission mechanism in GaN QDs by time-resolved photoluminescence (PL) measurements. The stacking of multiple layers is expected to influence the optical properties due the strain-induced realignment of dots in one level with respect to the adjacent level. The main motivation is to isolate pure dimensionality effects in the MQDs from the influence of the giant polarization (piezoelectric and spontaneous) induced electric fields present in the SQD system.[10−12] We present the first report on exciton localization in vertically correlated GaN MQDs in the presence of built-in strain field.

* Corresponding author. E-mail: arup@unt.edu.

10.1021/nl048511x CCC: $30.25
Published on Web 12/24/2004

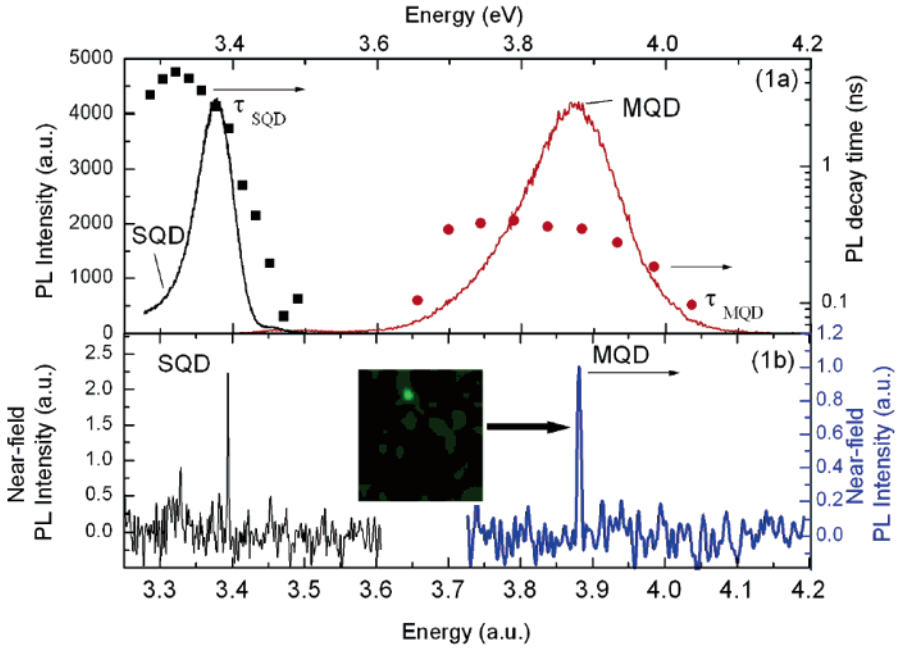

Figure 1. Comparison of PL spectra in single and stacked GaN QDs at 10 K: (a) time-integrated far-field PL, (b) near-field PL of a 450 nm × 450 nm scanned area, with spatial resolution of 40 nm, inset showing the spatially resolved PL of a MQD at 3.88 eV.

GaN dots were self-assembled on a 2 nm thin AlN layer over AlN/GaN superlattice buffer layer grown on sapphire substrate using molecular beam epitaxy.[8] Dots were self-assembled by nitridation using RF plasma in a nitrogen atmosphere. The dot size and density depend on the growth condition, deposition time, and post growth treatment.[9] The SQDs were allowed to ripen, unlike the MQDs, which were covered with a thin AlN spacer layer immediately after the nucleation of self-assembled GaN structures. The ripening of the dots in the SQDs leads to coupling in the lateral direction. AFM images show that SQDs has a relatively larger dot size (height/width − 20/150 nm) compared to the MQDs (8/40 nm). It is observed from high-resolution transmission electron microscopy that in SQDs, the lateral separation is about 2−4 nm, whereas in MQDs, the lateral separation is ∼ 4−5 nm in the cap layer and 5−8 nm in the underlying layers. Due to the narrower AlN spacer layers between the dots (∼2 nm), a stronger coupling exists between the dots in the vertical direction. Time-integrated PL (TI−PL) and time-resolved PL (TR−PL) measurements were performed using a frequency tripled Ti:sapphire laser mode-locked at 100 MHz with an excitation energy at 4.66 eV, and the PL signal was detected using a streak camera with a resolution of 15 ps. A near-field scanning optical microscope is used for studying exciton localization in single QD.

The recombination of the excitons has been investigated by TRPL measurements performed using a 100 MHz Kerr-lens mode-locked, frequency tripled Ti:sapphire laser with a typical temporal width of 80 fs and an average incident pump power of 0.3 mW (0.4 μJ/cm^2). The excitation wavelength was 270 nm (4.6 eV) and the PL signal was dispersed through a grating spectrometer (600 gr/mm) and measured using a Hamamatsu streak camera with a resolution of 15 ps.

The time integrated PL spectrum from a single QD layer was compared to a MQD sample measured 2−10 ns after the excitation of the pump laser pulse at 10 K (Figure 1a). The PL emission energy depends on the size of quantum dots. For MQDs with relatively smaller dots, the PL peak is at 3.86 eV, nearly 400 meV blue-shifted with respect to the bulk GaN bandedge. In SQDs, which are composed of larger dots due to the ripening effect, the PL peak is centered at 3.37 eV and is significantly red shifted from the MQD PL peak and lies 90 meV below the bulk GaN bandedge (3.46 eV). This red shift is a clear manifestation of the internal polarization-induced electric field present in wurtzite GaN QDs, which induces a red-shift in the QD transition energy due to quantum confined Stark effect. It appears in case of the single layer QDs owing to the relatively larger structural dimension, the induced electric field dominates the quantum confinement effect in larger QDs. The line width in SQDs is also considerably narrower due to the reduced dot distribution in a single period QD compared to that in the multilayered structure in MQDs. The line width in MQD is ≈200 meV compared to 70 meV for the SQDs, which clearly indicates that the dominant inhomogeneous broadening mechanism in the MQDs results from dot size variations from period to period. TEM images show vertical correlation in MQDs.[13] Figure 1b shows the near-field PL spectra of SQDs and MQDs consisting of dominant sharp spectral features respectively at 3.37 and 3.88 eV. The PL from a 450 nm × 450 nm area of MQD sample (inset of Figure 1b) shows that the emission area is less than 50 nm. The line width in SQD has a fwhm ∼ 0.9 meV compared to 2.3 meV in the MQD samples. The near-field PL peaks correspond to the central far-field emission energy from both SQDs and MQDs and indicates exciton localization in a cluster of few QDs. It is observed that the near-field PL line width shown in

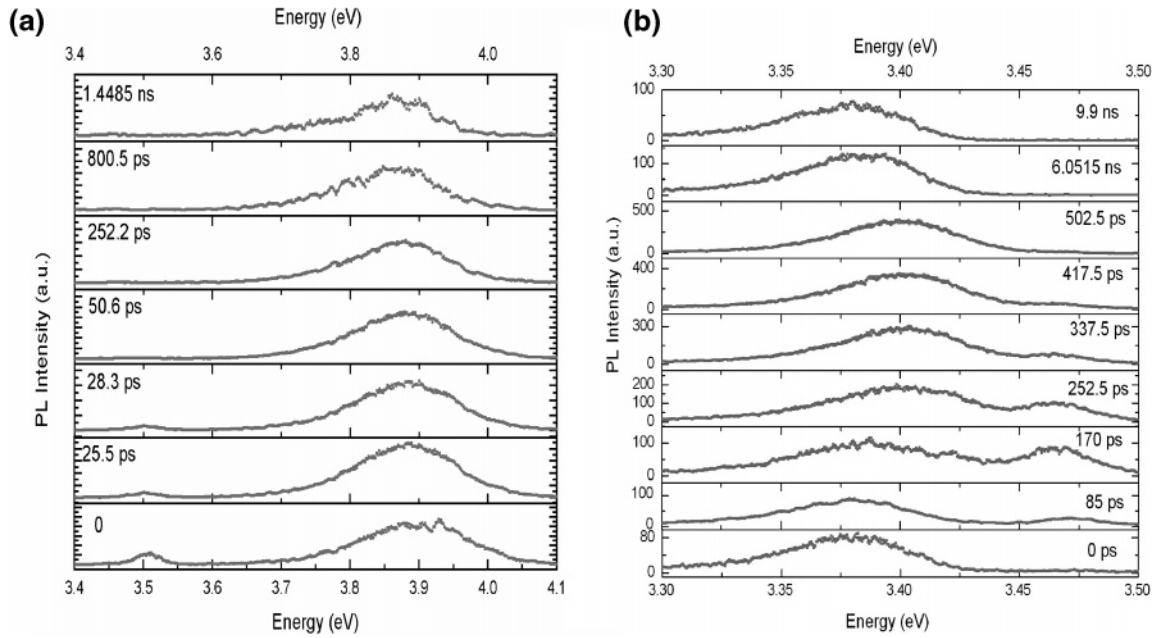

Figure 2. Time integrated photoluminescence spectra in (a) 20 period MQD and (b) SQD.

Figure 1b is significantly narrower than the far-field PL line width shown in Figure 1a. The narrow near-field PL spectrum ($\sim$ few meV) is presumably due to the emission from a cluster of 2−5 dots, which are excited by the narrow NSOM probe with 5 nm diameter and are 10−20 nm from the surface. The far-field PL is significantly broader ($>$ 100 meV) as it is influenced by inhomogeneous broadening due to emission from a large ensemble of QDs, which are simultaneously excited by a beam with relatively larger spot diameter. The near-field PL spectrum yields information on carrier recombination and exciton emission from single quantum dots with minimal inhomogeneous broadening due to lateral coupling. The far-field PL spectrum is strongly influenced by the lateral coupling in the GaN/AlN QD system with high dot density.

In MQDs, the lifetime is relatively steady (290−390 ps) across the PL peak as a result of the stronger carrier confinement in smaller QDs. Emission at lower energies arises from larger QDs with reduced wave function overlap and longer recombination times. Therefore, the decrease in τ_D at low emission energies is likely to be caused by nonradiative relaxation from the QDs. However, the decay from SQD is more complex due to the presence of a strain-induced piezoelectric polarization field. In SQDs, the lifetime varies by nearly 2 orders of magnitude ($\sim$70 ps to 5 ns), which indicates the presence of large intrinsic strain. At high emission energies, the GaN buffer layer at $\sim$3.46 eV acts as nonradiative recombination center. The strained and larger dots emitting at lower energies ($<$3.3 eV) also contribute to nonradiataive recombination and result in a decrease in the PL decay time in SQDs.

Figure 2a shows the temporal evolution of the PL spectrum from the 20-period QD sample measured at 10 K. A small peak emanates from the GaN buffer layer at 3.49 eV and decays within 25−30 ps. The PL spectrum is asymmetric and the decay constant shows a weak biexponential feature in all regions of this spectrum. With an increase in the delay time, a red shift of the PL peak exceeding 35 meV is observed, which indicates the collective effect of polarization fields and photoexcited carrier screening. QDs grown under reduced strain still have appreciable polarization fields present in the dot regions of the GaN/AlN MQDs. Under the influence of piezoelectric and spontaneous fields, optically excited carriers drift apart. The electrons (holes) move toward the direction opposed to (along) the piezoelectric/spontaneous field and the field induced by these spatially separated charge carriers will screen the piezoelectric/spontaneous field. On the other hand, the screening field due to spatially separated charge carriers decreases with the delay time due to the radiative recombination of electrons and holes. At $t_d = 0$, the screening field induced by the photoexcited electron and holes is the strongest, which reduces or partially balances out the piezoelectric and spontaneous field. As the delay time increases, carriers recombine radiatively and the screening field gradually diminishes and the original piezoelectric/spontaneous field is restored. Thus the total amount of shift from $t_d = 0$ to $t_d \rightarrow \infty$ effectively corresponds to the variation of the electron and hole levels in the presence of the piezoelectric/spontaneous field with and without carrier screening, respectively. The PL spectra from MQDs also show a strong confinement as indicated by the relatively small shift in the peak PL energy with temperature.[9]

Figure 2b shows the time-resolved spectra of the SQDs measured at various delay times at 10 K. Initially at $t = 0$, the time-integrated PL spectra show a single peak at 3.37 eV emitting from the single-period GaN QD dots at an energy below the GaN bandedge (Figure 1). The excitonic peak from the 3D-GaN buffer layers appears due to carrier relaxation from smaller dots relaxing carriers from higher energy states. Within 100 ps, carrier relaxation occurs from the bulk GaN states either due to the presence of shallow-

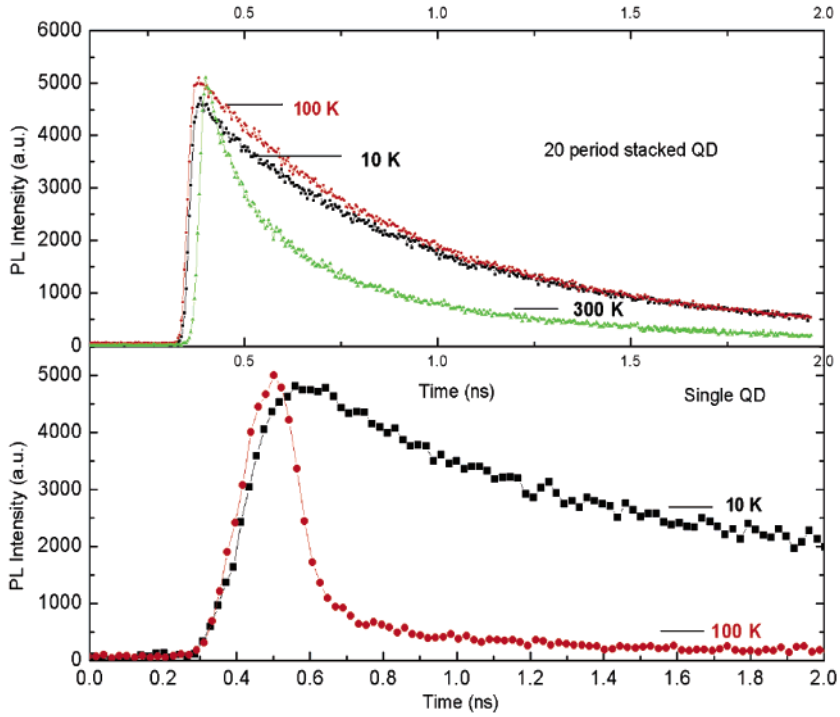

Figure 3. Comparison of temperature dependence of decay times in single and multiple quantum dots.

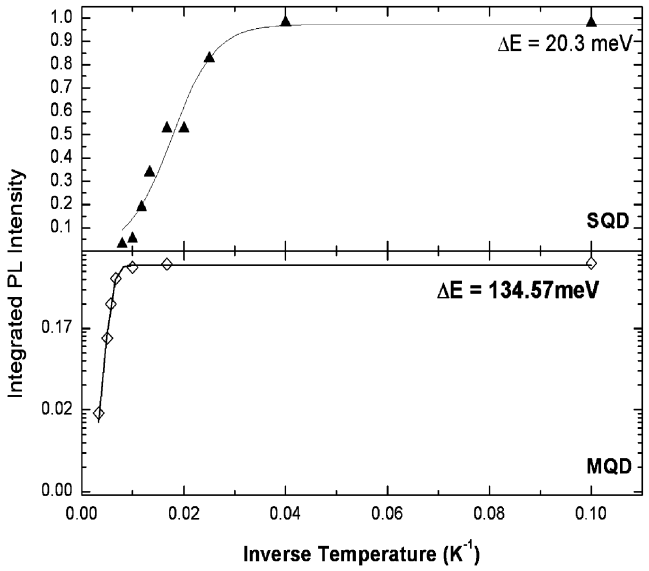

Figure 4. Spectrally integrated intensities and time-integrated data plotted as a function of inverse temperature.

level defect states or through the smaller GaN dots with size comparable to GaN bandedge emission energy. The TRPL decay time constant of the carriers at this energy (~3.45 eV) is extremely fast and occurs within 100 ps even at low temperature. This enhancement of the recombination rate is possibly due to the increase in the nonradiative recombination center that occurs due to this particular growth technique. We also observe an initial blue shift due to the band filling of the QDs and screening of the photoexcited followed by the gradual restoration of the large built-in piezoelectric field.[14] This time evolution also shows that the piezoelectric field is considerably larger in SQDs compared to MQDs. The relatively long decay time in single layer QDs at low temperature is a signature of the spatial separation of electron hole wave functions due to the strained induced by the ripening of the QDs during the growth process.[15]

A comparison of the temperature dependent spectrally integrated decay characteristics of the SQDs and MQDs been shown in Figure 3. In MQDs there is no significant difference in the decay constants from 10 to 100 K, and even at 300 K the nonradiative recombination rate is lower than that in a single period QD at 100 K. It is observed that in SQDs the nonradiative recombination process is dominant as the temperature increases and the PL intensity drops exponentially, unlike the temperature insensitive feature in MQDs.

To compare the effective binding energies of the excitonic states in confined QDs in the stacked MQDs and highly strained SQDs, we show in Figure 4 the normalized intensities of the time integrated spectral features as a function of inverse temperature. These intensities are successfully modeled with the activated behavior,

$$I(T) = I_o/[1 + C\exp(-\Delta E/k_B T)] \quad (1)$$

where ΔE is the activation energy.

The exciton recombination time in the GaN SQDs at 10 K is single exponential with an extraordinarily long exciton recombination time, ~5 ns and $\Delta E = \Delta E_{sqd}$ ~20 meV, while in MQDs $\Delta E = \Delta E_{mqd} \sim 134$ meV for the broad emission states. This shows that the emission associated with these QDs, whose activation energies differ by 6-fold, are significantly different. The intensities obtained from fits of the exponential decays in Figure 3 and Figure 1 also shows that the short-lifetime component corresponds to the broad emission feature in MQDs, while the long-lifetime component corresponds to the relatively narrower spectral feature

in SQDs. The PL spectra in SQD clearly result from excitons confined to the QDs. However, this state is only weakly bound (20 meV) and thermally depopulates by 150 K. The extraordinarily long lifetime of this state ($\sim$ 5.0 ns) indicates that the overlap of the electron (e) and hole (h) wave functions is significantly weaker than for the short-lived states in strongly confined smaller QDs in the stacked MQD system, suggesting that this excitonic state in SQD may result from spatially indirect e−h transitions. In contrast, these spectra and lifetimes indicate that the state responsible for the broad emissions in MQDs is strongly bound (134 meV) and persists nearly to room temperature. Moreover, the short lifetime of this PL emission indicates that the electron and hole overlap is large and the radiation recombination process is dominant.[17] The relatively long radiative lifetime in SQDs can also be attributed to the lack of additional decay channels induced by vertical correlation in MQDs.

The presence of a piezoelectric field in these larger clusters of SQDs is further supported by optical power dependence of the luminescence spectra. It has been observed (which is not shown here) that as excitation power density increases, the PL peak blue shifts significantly. This behavior is typical of piezoelectric nanostructures and is due to partial screening of the piezoelectric field by the photoexcited e−h pair.[16] A 25 meV blue shift is observed as the power density varies from 1 to 10 μJ/cm^2.

In conclusion, we have compared the carrier recombination dynamics in SQD and MQDs. It is observed that at low temperatures the recombination time in SQDs is over an order of magnitude longer than the nonradiative recombination process at 100 K. The vertical correlation among the adjoining stacked layer leads to enhanced PL efficiency in MQDs and results in an efficient emission at room temperature. At low temperature, the luminescence decay is dominated by radiative recombination with relatively shorter lifetimes (250−500 ps), which indicates a potential for device applications. In SQDs, nonradiative processes resulting in an extremely short total decay time constants at high temperatures dominate exciton recombination.

Acknowledgment. The authors are thankful to Dr. Brian P. Gorman for transmission electron microscopy of the quantum dot structures. This research was supported by the University of North Texas "Faculty Research Grants Program".

References

(1) Morkoç, H. *Nitride Semiconductors and Devices*; Springer-Verlag: Heidelberg, 1999. Nakamura, S.; Fasol, G. *The Blue Laser Diode*; Springer-Verlag: Heidelberg, 1997.
(2) Widmann, F.; Simon, J.; Daudin, B.; Feuillet, G.; Rouvière, J. L.; Pelekanos, N.; Fishman, G. *Phys. Rev. B* **1998**, *58*, R15989; Widmann, F.; Simon, J.; Pelekanos, N. T.; Daudin, B.; Feuillet, G.; Rouviere, J. L.; Fishman, G. *Microelectronic J.* **1999**, *30*, 353.
(3) Widmann, F.; et al. *Phys. Rev. B* **1998**, *58*, R15989. Widmann, F.; et al. *Microelectron. J.* **1999**, *30*, 353.
(4) Arakawa, Y.; Someya, T.; Tachibana, K. *Phys. Status Solidi B* **2001**, *224*, 1.
(5) Tanaka, S.; Takeuchi, M.; Aoyagi, Y. *Jpn. J. Appl. Phys.* **2000**, *39*, L831.
(6) Huang, D.; Fu, Y.; Morkoç, H. "Preparation, Structural and Optical Properties of GaN based quantum dots" in *Optoelectronic Properties of Semiconductor Nanostructures*; Steiner, T., Ed.; Artech House: Boston, 2004.
(7) Reshchikov, M. A.; Cui, J.; Yun, F.; Visconti, P.; Nathan, M. I.; Molnar, R.; Morkoç, H. *Mater. Res. Soc. Symp. Proc.* **2001**, *639*, G11.2.
(8) Morkoç, H.; Neogi, A.; Kuball, M. *Mater. Res. Soc. Proc.* **2004**, *749*, T6.5.1/N8.5.1/Z6.5.1.
(9) Neogi, A.; Everitt, H. O.; Morkoç, H.; Kuroda, T.; Tackeuchi, A. *IEEE Trans. Nanotechnol.* **2004**, *2*, 450.
(10) Woggon, U. *Optical Properties of Semiconductor QDs*; Springer: Berlin, 1997.
(11) Lipsanen, H.; Sopanen, M.; Ahopelto, J. *Phys. Rev. B* **1995**, *51*, 13868.
(12) Chamard, V.; Metzger, T. H.; Daudin, B.; Adelmann, C.; Mula, G. *Appl. Phys. Lett.* **2001**, *79*, 1971.
(13) Neogi, A.; Gorman, B. P.; Morkoç, H.; Kawazoe, T.; Ohtsu, M. Near-field Optical Spectroscopy and Microscopy of Self-assembled GaN/AlN Nanostructures. *Appl. Phys. Lett.* **2005**, in press.
(14) Talierco, T.; Lefebvre, P.; Gallart, M.; Morel, A. *J. Condens. Matter Phys.* **2001**, *13*, 7027.
(15) Andreev, A.; Reily, E. O. *Appl. Phys. Lett.* **2001**, *79*, 521.
(16) Shin, E.; Li, J.; Lin, J. Y.; Jiang, H. X. *Appl. Phys. Lett.* **2000**, *77*, 1170.
(17) Reale, A.; Massari, G.; Di Carlo, A.; Lugli, P.; Vinattieri, A.; Alderighi, D.; Colocci, M.; Semond, F.; Grandjean, N.; Massies, J. Comprehensive description of the dynamical screening of the internal electric fields of AlGaN/GaN quantum wells in time-resolved photoluminescence experiments. *J. Appl. Phys.* **2003**, *93*, 400.

NL048511X